

Organic Chemistry



In Situ Mass Spectrometric and Kinetic Investigations of Soai's Asymmetric Autocatalysis

Oliver Trapp,^{*,[a, b]} Saskia Lamour,^[a, b] Frank Maier,^[a] Alexander F. Siegle,^[a] Kerstin Zawatzky,^[a] and Bernd F. Straub^[c]*Dedicated to Prof. Dr. Volker Schurig on the occasion of his 80th birthday*

Abstract: Chemical reactions that lead to a spontaneous symmetry breaking or amplification of the enantiomeric excess are of fundamental interest in explaining the formation of a homochiral world. An outstanding example is Soai's asymmetric autocatalysis, in which small enantiomeric excesses of the added product alcohol are amplified in the reaction of diisopropylzinc and pyrimidine-5-carbaldehydes. The exact mechanism is still in dispute due to complex reaction equilibria and elusive intermediates. In situ high-resolution mass spectrometric measurements, detailed kinetic analyses and doping with in situ reacting reaction mixtures show the transient formation of hemiacetal complexes,

which can establish an autocatalytic cycle. We propose a mechanism that explains the autocatalytic amplification involving these hemiacetal complexes. Comprehensive kinetic experiments and modelling of the hemiacetal formation and the Soai reaction allow the precise prediction of the reaction progress, the enantiomeric excess as well as the enantiomeric excess dependent time shift in the induction period. Experimental structural data give insights into the privileged properties of the pyrimidyl units and the formation of diastereomeric structures leading to an efficient amplification of even minimal enantiomeric excesses, respectively.

Introduction

Autocatalysis and in particular self-amplifying chemical processes are of great interest as they provide an explanation for the efficient replication of molecules with intrinsic error correction in general,^[1] and the appearance of mirror image molecules with the same handedness, namely homochirality. Such processes are of fundamental importance in symmetry breaking^[2] related to the emergence of life.^[3] In an asymmetric reac-


tion or catalysis, it is usually expected that the enantiomeric excess of the reagent or catalyst used will be transferred linearly to the product formation. Positive nonlinear effects,^[4] which means that the use of only enantiomerically enriched reagents or catalysts lead to a significant increase in the enantiomeric excess in the product, are rarely observed. Mechanistic explanations for such reactions with positive nonlinear effects were discussed by Kagan^[5] and Noyori.^[6,7] considering reversible monomer-dimer associations. Frank^[8] postulated a theoretical model leading to a spontaneous asymmetric synthesis. If dimers can be formed from their monomeric building blocks, for example, by intermolecular interactions, they are of the same configuration (homochiral) or of opposite configuration (heterochiral). Since these homochiral and heterochiral dimers are diastereomeric to each other, they have different intrinsic properties, which are reflected in their solubility, rate of formation and other physical properties. The formation of heterochiral dimers from an enantiomerically enriched mixture can increase the enantiomeric excess of the free monomeric major enantiomer.^[9]


In 1995, Soai^[10,11] reported an extremely remarkable reaction. When pyrimidine-5-carbaldehyde **4** reacts with diisopropylzinc (*i*Pr₂Zn) in the presence of a catalytic amount of pyrimidyl alcohol **1** with a low *ee*, asymmetric autocatalytic amplification of the enantiomeric excess gives the pyrimidine alcohol **1** with high *ee* as the final product (Scheme 1a). Autocatalysis and amplification are also observed in pyridyl-3-carbaldehydes,^[12] however the 2-alkynyl substituted pyrimidine analogues are

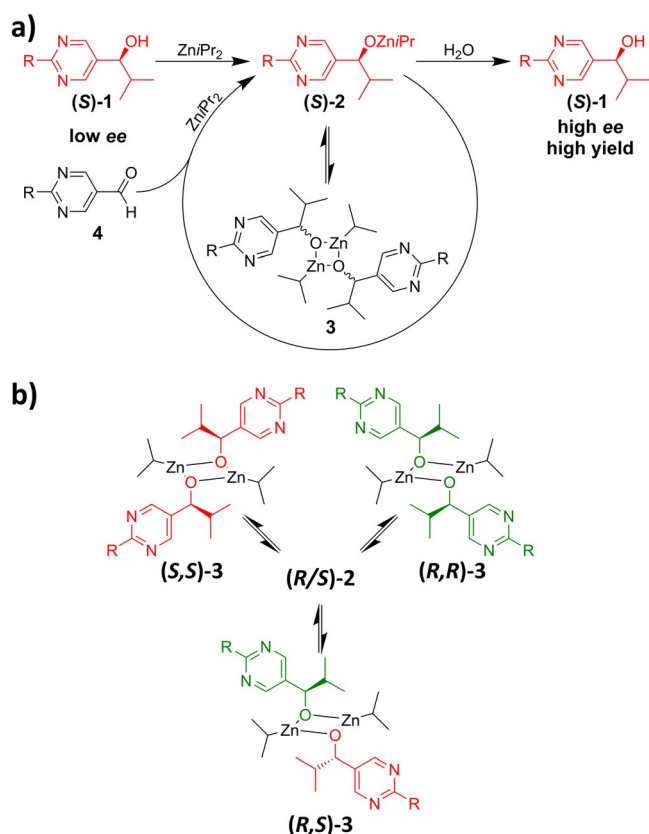
[a] Prof. Dr. O. Trapp, Dr. S. Lamour, Dr. F. Maier, Dr. A. F. Siegle, Dr. K. Zawatzky
Department of Chemistry
Ludwig-Maximilians-University Munich
Butenandtstr. 5-13, 81377 Munich (Germany)
E-mail: oliver.trapp@cup.uni-muenchen.de

[b] Prof. Dr. O. Trapp, Dr. S. Lamour
Max-Planck-Institute for Astronomy
Königstuhl 17, 69117 Heidelberg (Germany)

[c] Prof. Dr. B. F. Straub
Organisch-Chemisches Institut
Ruprecht-Karls-Universität Heidelberg
Im Neuenheimer Feld 270, 69120 Heidelberg (Germany)

 Supporting information and the ORCID identification number(s) for the author(s) of this article can be found under:
<https://doi.org/10.1002/chem.202003260>.

 © 2020 The Authors. Published by Wiley-VCH GmbH. This is an open access article under the terms of Creative Commons Attribution NonCommercial License, which permits use, distribution and reproduction in any medium, provided the original work is properly cited and is not used for commercial purposes.



Scheme 1. Soai's asymmetric autocatalytic reaction. a) Conversion of pyrimidine-5-carbaldehyde **4** with diisopropylzinc (iPr_2Zn) in the presence of a catalytic amount of pyrimidyl alcohol **1**. b) Formation of homochiral **(R,R)-3**/**(S,S)-3** and heterochiral **(R,S)-3** dimers of the isopropylzinc pyrimidyl alkoxides **2**. *The dimers can exchange their monomeric moieties without formation of the monomers **2**.^[32] $\text{R} = (\text{H}_3\text{C})_3\text{C}-\text{C}\equiv\text{C}-$.

superior in amplification of the ee. Even a trace imbalance of chiral molecules^[13] such as an extremely low ee of the initial catalyst of only $\sim 5 \times 10^{-5}\%$ ^[14] or other chiral triggers like $^1\text{H}/^2\text{H}$,^[15] $^{12}\text{C}/^{13}\text{C}$,^[16] $^{14}\text{N}/^{15}\text{N}$ ^[17] and $^{16}\text{O}/^{18}\text{O}$ ^[18] isotopically labelled cryptochiral compounds,^[19] cryptochiral compounds,^[20] circularly polarized light,^[21] (enantiomorph) crystals^[22] and other compounds^[23] are able to induce enantioselectivities, that lead to an amplification greater than 99.5% ee in a few cycles. A highly interesting feature of the reaction is, that spontaneous symmetry breaking with stochastic distribution of the final **(R)-1** or **(S)-1** product is possible, even when no chiral additive is employed.^[24]

Numerous findings and reports contributed to the mechanistic understanding of the Soai reaction.^[2] Still, open questions remain, especially regarding (a) the origin of enantioselectivity, (b) kinetic aspects of the reaction, that is, the reliable prediction of the chiral amplification, and (c) the privileged structure of the pyrimidyl-5-carbaldehydes and corresponding alcohols. While the last point (c) can be explained by experimental findings of similar reactions with the possible coordination of the nitrogen containing pyridyl or pyrimidyl rings and the associated activation of the alkyl zinc compounds as well as the formation of supramolecular structures,^[6a] points a) and

b) are not that obvious. The elucidation of the mechanism is highly challenging due to complex reaction equilibria and elusive intermediates.^[25–29] It is well established that isopropylzinc pyrimidyl alkoxides **2** can form dimers, tetramers^[30,31] and oligomeric compounds.^[2] The dimers can be either homochiral (**(R,R)-3** or **(S,S)-3**) or heterochiral (**(R,S)-3**) (Scheme 1b).^[32] It is important to note, that the interconversion of the dimers **3** can proceed by direct exchange of the monomeric moieties without formation of the monomers.^[32] The implication of this equilibrium is, that the equilibrium constant for the heterochiral dimer formation K_{hetero} is twice the equilibrium constant for the homochiral dimer formation $K_{\text{hetero}}/K_{\text{homo}} = 2$.^[33] Thus, non-linear effect can be well explained, because an imbalance of the enantiomers leads to amplification as soon as more stable heterochiral dimers **(R,S)-3** have formed. Blackmond and Brown developed a model considering dimers **3** as catalytically active species based on reaction progress analysis by calorimetric measurements and NMR spectroscopy. These dimers, tetramers^[30,31] and oligomers^[34] were characterized by comprehensive NMR spectroscopic measurements and single-crystal X-ray diffraction analysis,^[35] and these findings are supported by quantum chemical computations.^[36] Kinetic studies corroborate these results with pronounced effects of the additive concentration^[37] and ee leading to an induction period and a sigmoidal kinetic profile typical for autocatalytic processes.^[2] Schiaffino performed quantum chemical calculations of the kinetic constants at the M05-2X/6-31G(d) level of theory and investigated the effect of the aza group in the pyrimidine moiety to activate the zinc reagent in the tetrameric complex.^[38]

In 2012 Brown, Blackmond and co-workers^[39] reported the identification of a transient hemiacetal intermediate in the Soai reaction of 2-(adamantylacetylene-1-yl)pyrimidine-5-carbaldehyde and 2-(adamantylacetylene-1-yl)pyrimidyl alcohol by ^1H NMR spectroscopic kinetic studies. Gridnev and Vorobiev investigated by quantum chemical DFT calculations and kinetic analysis potential acetal intermediates. They concluded that the acetals are off-loop species because they are not precursor of the reaction product.^[27] In this context, another highly remarkable discovery was reported by Hawbaker and Blackmond, where hydroxy ethers interfere with the Soai reaction and even inhibit the reaction.^[19]

More recently, Denmark and co-workers^[40] performed investigations of the Soai reaction with focus on the role of the nitrogen atoms in the pyrimidine/ pyridyl moiety, the structure of the Zn-alkoxides in solution by NMR spectroscopic studies and in situ IR kinetic studies using pyridyl-3-carbaldehyde as surrogate, (“Trojan-Horse” substrate). An alternative mechanism is proposed, considering a “cube escape” model. Such cube-type structures were also proposed by Noyori and co-workers^[6a] in the enantioselective addition of dialkylzincs to aldehydes promoted by chiral β -amino alcohols, that is, (–)-3-*exo*-(dimethyl-amino)isoborneol (DAIB) and has been discussed by Brown and co-workers in the context of the Soai reaction as potential tetrameric structure of the Zn-alkoxides.^[25]

Furthermore, the Soai reaction shows some peculiarities that are well documented, but still unexplained such as (a) an un-

usual inverse temperature dependence on the reaction kinetics, that is, the maximum reaction rate increases significantly as the reaction temperature is decreased,^[41] and (b) a prolonged induction period, which are not yet rationalized by properties of potential catalyst structures or corresponding kinetic models. Herein, we seek to investigate the open mysteries of Soai's asymmetric autocatalysis.

Results and Discussion

First, we performed reaction kinetic investigations using multiplexing HPLC^[42] in the flow-injection mode^[43] (Chiralpak IB, mobile phase *n*-hexane/THF 55:45, 1.2 mL min⁻¹), which provides temporal resolution of the stereoisomers formed (Figure 1 in the Supplementary Information). Reaction progress was observed injection of sample pulses with a time interval of 2.1 min from the reaction mixture onto the chiral separation column (Figure 1 a and b). We systematically varied the concentrations of the reactants and additives of the Soai reaction (2-(*tert*-butylacetylene-1-yl)pyrimidyl-5-carbaldehyde **4**: 10.6–41 mM, ((*R*)-2-(*tert*-butylacetylene-1-yl)pyrimidyl-5-(*iso*-butan-1-ol) (**R**)-1 (*ee* > 99.9%): 0.266–4 mM; *i*Pr₂Zn: 30–130 mM (Figure 1 b and Figures S6–S23 in the Supporting Information).

Kinetic analysis of these data gives a reaction order of 1.9 in [**4**], an order of 1 in [**1**], and an order of 0 in [*i*Pr₂Zn] (Figures 24–26 in the Supplementary Information), confirming previous studies [Eq. (1)].^[41]

$$\frac{d[1]}{dt} = k[4]^{1.9}[1][iPr_2Zn]^0 \quad (1)$$

Surprisingly, when we performed the HPLC separation of the reaction mixture using isopropanol instead of THF in the mobile phase we observed the enantiomers of another compound connected by plateau formation with **4**. We identified these peaks as the isopropyl hemiacetals (**R**)-**5**_{*i*Pr} or (**S**)-**5**_{*i*Pr} (Figure 2 a), that is, in the case of chiral alcohols diastereomeric hemiacetals are expected (vide infra).

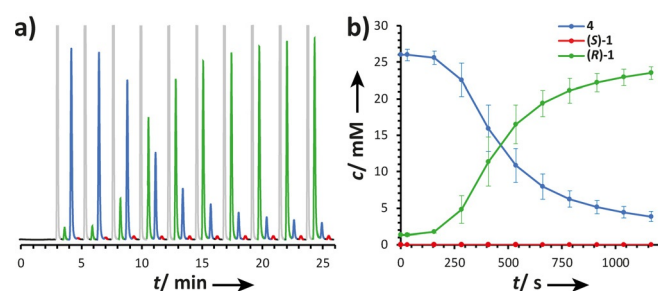


Figure 1. a) Reaction progress analysis by flow-injection analysis using enantioselective HPLC to separate the reactant **4** and product enantiomers (**R**)-**1** (green) and (**S**)-**1** (red). Reaction conditions: 26.0 mM 2-(*tert*-butylacetylene-1-yl)pyrimidyl-5-carbaldehyde **4**, 1.3 mM (*R*)-2-(*tert*-butylacetylene-1-yl)pyrimidyl-5-(*iso*-butan-1-ol) (**R**)-**1** (*ee* > 99.9%) and 40 mM *i*Pr₂Zn in toluene (grey) at 20 °C. Separation conditions: Chiralpak IB column (25 cm, I.D. 4.6 mm, particle size 5 μm), *n*-hexane/THF 55:45 (v/v), 1.2 mL min⁻¹. b) Concentration of (**R**)-**1**, (**S**)-**1** and **4** vs. time *t*.

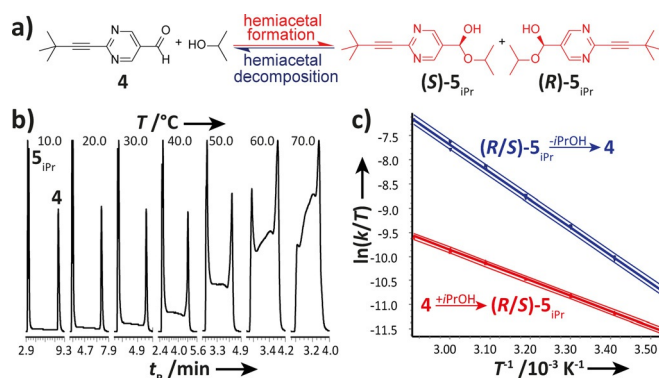


Figure 2. a) Hemiacetal formation of **4** in presence of *i*-propanol. b) Temperature-dependent enantioselective DHPLC measurements of the formation of the hemiacetal **5**_{*i*Pr} with isopropanol (Chiralpak IC-3 (15 cm, I.D. 4.6 mm, particle size 3 μm), *n*-hexane/isopropanol 60:40 (v/v), 1.0 mL min⁻¹). c) Eyring plot for the determination of the activation parameters ΔH^\ddagger and ΔS^\ddagger of the hemiacetal formation (red data points) and the hemiacetal decomposition (blue data points) obtained from the DHPLC experiment. The upper and lower curves represent the error bands (21 data points each) of the linear regression with a level of confidence of 95%.

Remarkably, these hemiacetals **5**_{*i*Pr} are subject to a dynamic interconversion, which we investigated by temperature-dependent enantioselective dynamic HPLC (DHPLC)^[44,45] (Figure 2 b and Figures S28–S35 in the Supporting Information).

The thermodynamic parameters of the formation of the hemiacetal **5**_{*i*Pr} were determined by linear regression of the thermodynamic Gibbs free energies $\Delta G(T)$, obtained from the equilibrium constants *K*, vs. the temperatures *T* (correlation coefficient *r* = 0.9949) to be $\Delta G^0 = 3$ kJ/mol, $\Delta H^0 = -15.6$ kJ/mol and $\Delta S^0 = -62.5$ J/(Kmol) (Figure S36 in the Supporting Information).

The activation enthalpies ΔH^\ddagger for the hemiacetal **5**_{*i*Pr} formation and decomposition were obtained via the slope and the activation entropies ΔS^\ddagger via the intercept of the Eyring plots ($\ln(k/T)$ vs. $1/T$) (Figure 2 c). Deviations of the activation parameters ΔH^\ddagger and ΔS^\ddagger have been calculated by error band analysis of the linear regression with a level of confidence of 95%. The activation parameters of the hemiacetal **5**_{*i*Pr} formation are $\Delta H^\ddagger = 26.3 \pm 0.2$ kJ mol⁻¹ and $\Delta S^\ddagger = -195 \pm 34$ J/(Kmol) (*r* = 0.9990, residual deviation *s_y* = 0.0306) and the hemiacetal **5**_{*i*Pr} decomposition are $\Delta H^\ddagger = 47.7 \pm 0.2$ kJ mol⁻¹ and $\Delta S^\ddagger = -112 \pm 1$ J/(Kmol) (*r* = 0.9994, *s_y* = 0.0630). The formation of hemiacetal **5**_{*i*Pr} from **4** is endergonic, however this is a highly dynamic process and interestingly, the kinetic parameters $k_1(293$ K) = 4.1×10^{-3} (mol s⁻¹) and $k_{-1}(293$ K) = 1.3×10^{-2} s⁻¹. Hemiacetals, formed from the pyrimidine-5-carbaldehyde and its corresponding alcohol can function as a transient chiral ligand to activate the dialkylzinc reagent, very similar to the β-dialkylaminoalcohols in Noyori's DAIB catalysis^[6a] or Blackmond's hydroxy ethers.^[19] The in situ formation of a transient catalyst by reaction or interaction of molecules participating in the reaction is a fundamental mechanism leading immediately to autocatalysis and amplification. Similar mechanisms are well known in substrate activated enzyme catalysis to regulate biochemical reaction networks and in artificial systems.^[46] Furthermore, the

thermodynamic data indicate that the formation of the hemiacetal is favored at lower temperature and if it is involved in the autocatalytic cycle, it correlates with the observation that the Soai reaction is accelerated at lower temperature. Moreover, the measured reaction kinetics of the formation of the hemiacetals agrees with the observed induction period of the Soai reaction.

^1H NMR spectroscopic studies in CD_3OD reveal that the electron-deficient pyrimidine moiety of **4** and the unsubstituted pyrimidyl-5-carbaldehyde **4_H** promote the formation of deuterated methyl hemiacetals (characteristic hemiacetal proton at $\delta = 5.7$ ppm; cf. Figures S39 and S42 in the Supporting Information) in 95% yield at room temperature, while for comparison benzaldehyde yields only 9% (Table S4 in the Supporting Information). Temperature dependent measurements confirm the trend that the hemiacetal formation is favored at lower temperature (Figures S40 and S41 in the Supporting Information). This formation of hemiacetals is also observed in toluene, the solvent used in the Soai reaction: Reaction of **4** and **4_H** with *rac*-2-methyl-1-phenylpropan-1-ol in $[\text{D}_8]$ toluene give diastereomeric hemiacetals in 11% and 9% yield, respectively. More important, the diastereomeric ratio of 1:2.6 for the unsubstituted pyrimidine hemiacetal improves to 1:5.2 for the 2-(*tert*-butylacetylene-1-yl) substituted pyrimidine hemiacetal (HSQC spectra depicted in Figures S43 and S44 in the Supporting Information). In this context, it is important to note that the formation of stereolabile hemiacetals offers the conceptual mechanism of minor enantiomer recycling^[47] leading to the amplification of the major enantiomer/ diastereoisomer. In the next step, we investigated the Soai reaction by in situ high-resolution mass spectrometric experiments. In these experiments there is no separation column involved to avoid

quenching of the reaction intermediates. We monitored the course of the Soai reaction under inert conditions (anhydrous toluene, argon atmosphere) by feeding the reacting reaction mixture continuously (10 $\mu\text{L}/\text{min}$) but pulsed (time interval of 30 s) via a 5 μL sample loop of a 6-port valve (anhydrous toluene as eluent, flow rate 200 $\mu\text{L}/\text{min}$) into a high-resolution Orbitrap mass spectrometer (Figure S45 in the Supporting Information) using atmospheric pressure chemical ionization (APCI) under mild ionization conditions ($T = 150^\circ\text{C}$, N_2).

To identify all intermediates and transient intermediates during the Soai reaction, all pulsed injections were summed up over the complete reaction progress and the mass range between m/z : 180 and 800 in a first step (Figure 3a; Figures S46–49 in the Supporting Information). This mass spectrum shows the complexity of intermediates formed in the Soai reaction. We identified (cf. Figure 3b) the alcohol **1a** and its fragment **1b**, the monomeric Zn-alkoxides **2a** and **2b**, the dimeric Zn-alkoxides **3a** and **3b** (different charge states), pyrimidine-5-carbaldehyde **4**, the Zn-complex of the hemiacetalate **5a**, the hemiacetal fragments **5b** and **5c**, a hydroxylated structure **5d**, which is probably formed by the ionization process, hemiacetal **5e** with $i\text{Pr}_2\text{Zn}$ coordinated to it (this can be bridged or open), the hemiacetalate with coordinated toluene **5f**. Structures **7a–7d** are Zn-hemiacetalate complexes with another molecule or fragment of alcohol **1** coordinated, and structure **8** represents a dimeric Zn-hemiacetal complex.

The identification of the Zn complexes is facilitated by the characteristic isotope pattern of Zn (Figure 4a, right MS spectrum); for comparison, the high-resolution MS spectrum on the left side in Figure 4a shows the formation of hemiacetal **5** (m/z 421.25822) by mixing **1** and **4** in toluene. High-resolution MS spectra of the identified structures are depicted in Fig-

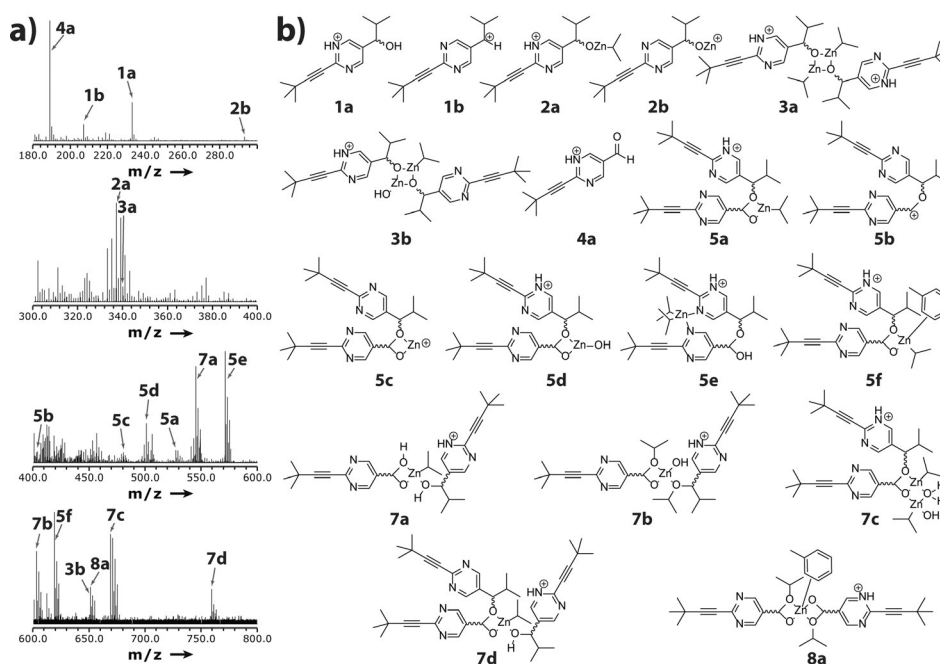


Figure 3. Identification of intermediates and transient intermediates of the Soai reaction by in situ high-resolution mass spectrometry. a) Summarized mass spectra and assigned peaks covering m/z 180–800. b) Structures identified by high-resolution MS.

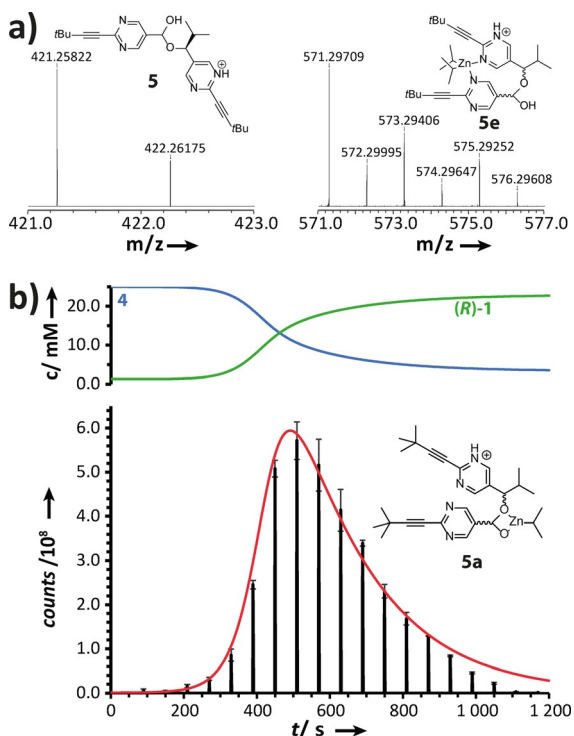


Figure 4. Investigation of the Soai reaction by in situ high-resolution mass spectrometry. a) High-resolution mass spectrum of the hemiacetal **5** (left) and transient hemiacetal structure **5c** (right) obtained by in situ MS reaction monitoring of the Soai reaction. b) Monitoring of the ion counts (bottom) of **5a** (m/z 527.234115) and **5e** (m/z 571.297085) vs. time during the Soai reaction (top). Reaction conditions: 25.0 mM **4**, 1.25 mM (**R**-**1**) ($ee > 99.9\%$) and 50 mM iPr_2Zn in toluene at 20 °C.

ures S50–S63 in the Supporting Information. These structures were also confirmed by MS/MS measurements.

By the temporal resolution of the injection pulses in the experimental setup, the relative concentration of the transient hemiacetal intermediate **5** can be monitored in the course of the Soai reaction (Figure 4b). Interestingly, the apex of this profile coincides with the inflection point of the sigmoidal kinetic profile of the Soai reaction (Figure 4b, top), which suggests, that the transient Zn–hemiacetalate **5** is slowly built up during the induction period, is then amplified in the autocatalytic cycle and finally depleted.

The coordination of iPr_2Zn to the *N* atoms of the pyrimidine rings not only activates the zinc reagent, but also favors the formation of hemiacetals by spatial arrangement (tweezer effect) and electronic effects. Interestingly, no bridged pyrimidyl alcohols **1**, pyrimidyl alkoxides **2** or pyrimidine-5-carbaldehydes **4** are observed, which can be attributed to the noncovalent nature of such complexes, which are not stable under the conditions of the APCI.

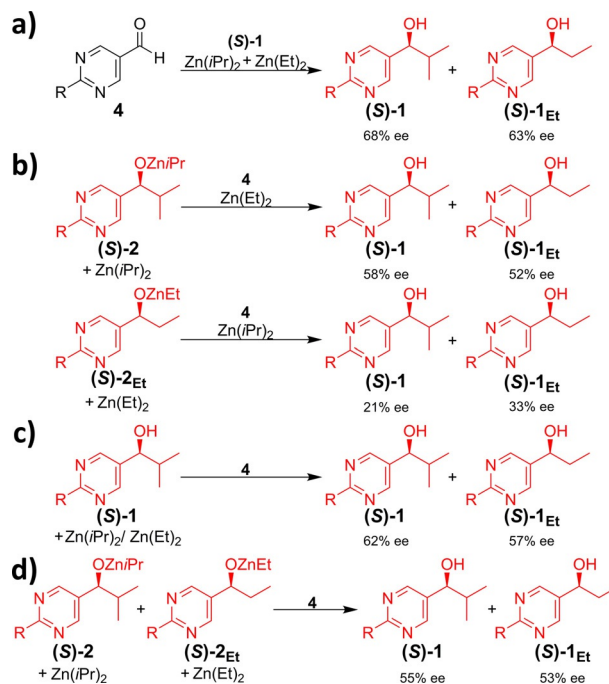
To investigate the role of the dialkylzinc reagent and the alcohol additive in the Soai reaction we performed mixing experiments. We systematically varied iPr_2Zn and diethylzinc (Et_2Zn) as reagent in the reaction itself and to pre-form Zn-alkoxides **2**.

In a second set of experiments we mixed various concentrations of the additives (**S**-**1**), (**S**-**1**)_H and (**R**-**1**)_H to study the

effect on the ee . While in the Soai reaction of **4** with Et_2Zn only low ee values are observed, the reaction with a 1:1 mixture of iPr_2Zn and Et_2Zn (**S**-**1**) gives ee values of 68% and 63% for (**S**-**1**) and (**S**-**1**)_{Et}, respectively (Scheme 2a).

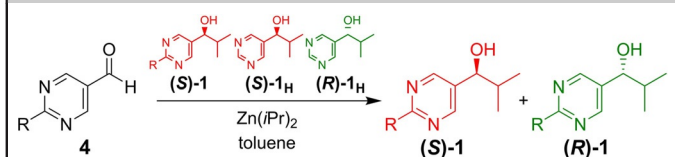
If the reaction is started with pre-formed (**S**-**2**) or (**S**-**2**)_{Et}, higher ee values are observed for the isopropyl substituted alkoxide (**S**-**2**) compared to the ethyl substituted alkoxide (**S**-**2**)_{Et} (Scheme 2b). If iPr_2Zn , Et_2Zn and (**S**-**1**) are pre-mixed, the selectivity of the isopropyl substituted alkoxide (**S**-**2**) dominates and gives higher ee values (Scheme 2c). This is also observed for the competitive reaction using (**S**-**2**) and (**S**-**2**)_{Et} simultaneously (Scheme 2d). These experiments show that the catalyst formed in the induction period strongly depends on the starting conditions and remains catalytically active and selective throughout the Soai reaction.

This becomes evident from the mixing experiment where the concentrations of the additives (**S**-**1**), (**S**-**1**)_H and (**R**-**1**)_H are varied. The 2-(*tert*-butylacetylene-1-yl) substituted alcohol (**S**-**1**) dominates the selectivity, resulting in high ee values (Table 1). Entries 4 and 5 of Table 1 show, that the catalyst formed from additive (**S**-**1**) remains catalytically active and the selectivity is controlled by the catalyst, which is better stabilized in solution. The 2-(*tert*-butylacetylene-1-yl) substituent improves the residence time and with that the turnover number. This explains also the excellent selectivities of the 2-(adamantylacetylene-1-yl)- and 2-(trimethylsilylacetylene-1-yl)-substituted pyrimidyl alcohols.^[10c,37] Furthermore these mixing experiments are in good agreement with the experiments by Amedjkouh using pyrimidine alcohol **1** as chiral additive in the Soai reaction of pyridyl-3-carbaldehydes.^[12d,48]



Scheme 2. Systematic variation of iPr_2Zn , Et_2Zn and the additives **1** or **2**. $R = -C\equiv C-C(CH_3)_3$.

Table 1. Variation of the additive composition in the Soai reaction^[a]



| Entry | (S)-1 [mol %] | (S)-1 _H [mol %] | (R)-1 _H [mol %] | % ee |
|-------|---------------|----------------------------|----------------------------|---------|
| 1 | 5.00 | – | – | 95 (S) |
| 2 | – | 5.00 | – | 47 (S) |
| 3 | 3.75 | 1.25 | – | 92 (S) |
| 4 | 1.25 | 3.75 | – | 80 (S) |
| 5 | 2.50 | – | 2.50 | 64 (S) |
| 6 | 1.67 | – | 3.33 | 26 (S) |
| 7 | 1.25 | – | 3.75 | 1.5 (R) |
| 8 | 1.00 | – | 4.00 | 14 (R) |
| 9 | 0.86 | – | 4.14 | 28 (R) |

[a] R = $-\text{C}\equiv\text{C}-\text{C}(\text{CH}_3)_3$

A doping experiment corroborates that the Soai reaction is catalyzed by a transient catalyst formed in the course of the reaction. For this purpose, we transferred the reaction solution of a running Soai reaction to a just started Soai reaction.

For this, four Soai reactions (25 mM 2-(*tert*-butylacetylene-1-yl)pyrimidyl-5-carbaldehyde **4**, 1.25 mM (*R*)-2-(*tert*-butylacetylene-1-yl)pyrimidyl-5-(*iso*-butan-1-ol) (*R*)-**1** ($ee > 99.9\%$), 20 °C, all concentrations are final concentrations after addition of the $i\text{Pr}_2\text{Zn}$ solution) were prepared from the same stock solutions and distributed in 4 vials under inert reaction conditions. 2 vials were used as reference vials, one started simultaneously (1st vial) with a 2nd vial, in which the transient catalyst is formed during the reaction (for experimental details a detailed timing Scheme is depicted in Figure S64 in the Supporting Information). The Soai reactions are started by addition of $i\text{Pr}_2\text{Zn}$ (125 mM final concentration). After 210 s the 3rd Soai reaction is started by addition of $i\text{Pr}_2\text{Zn}$ (125 mM final concentration). 218 s after the start of the reference reaction and the Soai reaction in the 2nd vial 60 μL of the reaction solution are transferred from the 2nd vial into the 3rd vial. The 2nd reference (4th vial) was started after the completion of reactions 1 and 2. All reactions were monitored by multiplexing HPLC in the flow-injection mode. Analysis of the kinetic data (Figure 5) shows, that the induction period is reduced in the doped experiment. Quantitative kinetic analysis confirms that the inflection point (maximum reaction rate) of the “normal” Soai reaction (25.0 mM **4**, 1.25 mM (*R*)-**1** ($ee > 99.9\%$) and 125 mM $i\text{Pr}_2\text{Zn}$ in toluene at 20 °C) is at 255 s with an initial reaction rate of $4.2 \times 10^{-3} \text{ mol s}^{-1}$, while in the doped experiment the inflection point is at 200 s and the initial reaction rate is $1.4 \times 10^{-2} \text{ mol s}^{-1}$ (Figures S65–S70 in the Supporting Information). The induction period is shifted by 55 s in the doped experiment. It has to be pointed out, that adding 60 μL of a completed Soai reaction does not influence the induction period.

Considering all kinetic and thermodynamic data of the hemiacetal formation, the structural information obtained by the in situ high-resolution mass spectrometric reaction monitoring, the transient formation of the Zn-hemiacetalate **5** during the

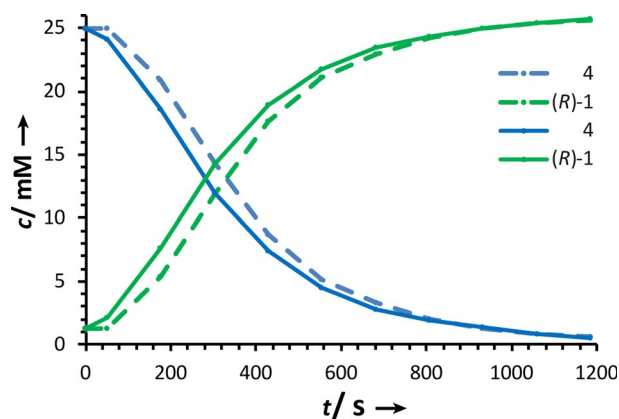
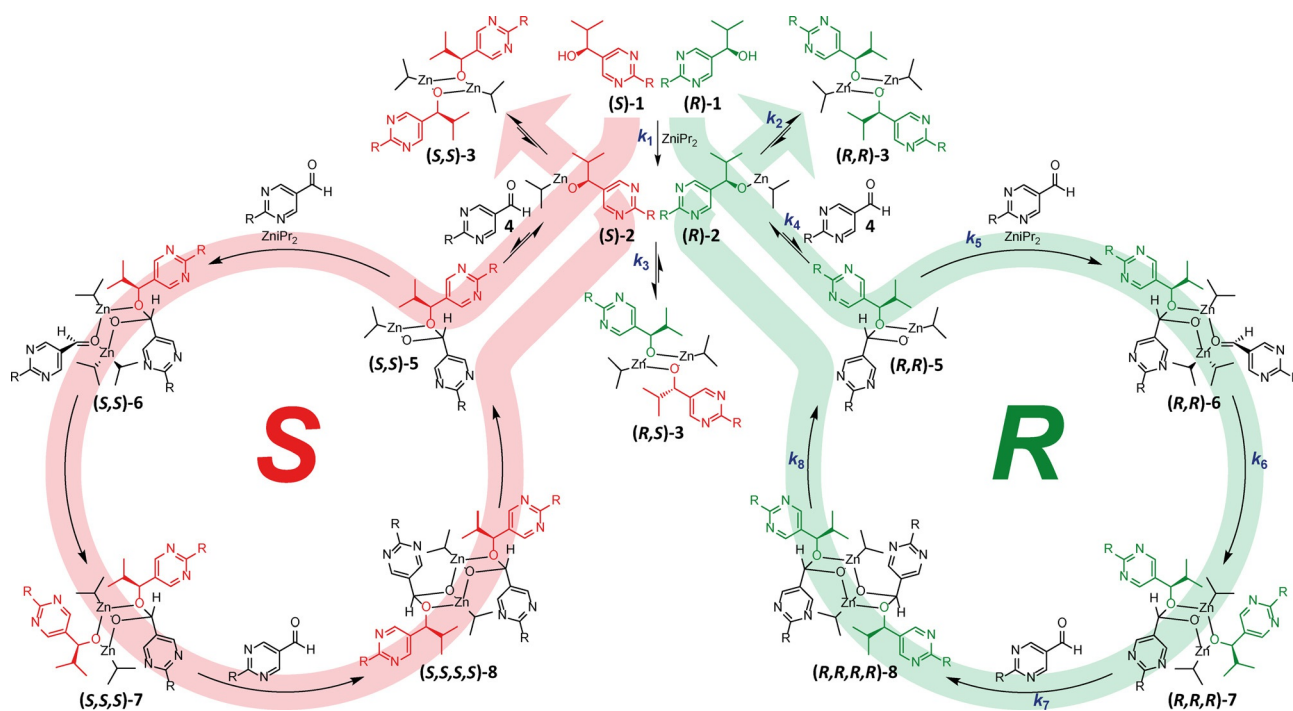


Figure 5. Reaction progress of concentrations (*R*)-**1** and **4** vs. time t of the doping experiment. The solid lines represent the Soai reaction doped with the transient catalyst solution (60 μL) formed from an immediately preceding ($t = 218$ s) Soai reaction. The dashed lines represent the reaction progress of the reference Soai reaction. Reaction conditions: 25.0 mM **4**, 1.25 mM (*R*)-**1** ($ee > 99.9\%$) and 125 mM $i\text{Pr}_2\text{Zn}$ in toluene at 20 °C.

Soai reaction, the mixing experiments and the doping experiment, we propose a reaction mechanism that can explain the high amplification of the experimentally observed enantioselectivity (Scheme 3). This mechanism starts with the formation of the isopropylzinc pyrimidyl alkoxides **2** from (*R*)-**1** and/ or (*S*)-**1**. The isopropylzinc pyrimidyl alkoxides **2** are in equilibrium with the homochiral (*R,R*)-**3**/ (*S,S*)-**3** and heterochiral (*R,S*)-**3** dimers. Depending on this first selection process the dominating enantiomer directs if the autocatalytic cycle proceeds to the right autocatalytic *R*-cycle (green) or the left autocatalytic *S*-cycle (red).

A key step is the formation of the transient hemiacetal catalyst **5**, which is in a dynamic equilibrium between the zinc alkoxide **2** and aldehyde **4** forming diastereomeric complexes (*R,R*)-**5** or (*R,S*)-**5**, if (*R*)-**1** dominates, or forming diastereomeric complexes (*S,S*)-**5** or (*S,R*)-**5**, if (*S*)-**1** dominates. These structures are very similar to the zinc β -dialkylaminoalcoholate structures in Noyori's DAIB catalyst.^[6a] DFT calculation at the PBE0-D3/ LACVP** level of theory as implemented in the Jaguar 10.1 quantum chemistry program package^[49–55] of optimized structures of (*R,R*)-**5** and (*R,S*)-**5** indicate that the diastereomer (*R,R*)-**5** is favored by 6 kJ mol⁻¹ (cf. Supporting Information, Figures S118 and S119). In the following only the autocatalytic *R*-cycle on the right side will be discussed, which is mirror-symmetrical to the autocatalytic *S*-cycle. In the next step of this cycle pyrimidine-5-carbaldehyde **4** and $i\text{Pr}_2\text{Zn}$ are coordinated to the hemiacetal (*R,R*)-**5** forming adduct (*R,R*)-**6**. This spatial alignment of the carbaldehyde results in a transfer of the adjacent isopropyl group from the *re* side giving (*R,R,R*)-**7**. DFT calculations provide an energy barrier of 54 kJ mol⁻¹ (cf. Supporting Information Figures S120–S123). Insertion of another molecule of the pyrimidine-5-carbaldehyde **4** leads to the dimeric hemiacetal (*R,R,R,R*)-**8**, which splits into two monomeric hemiacetals (*R,R*)-**5**, which explains the rapid sigmoidal increase in the formation of catalytically highly active (*R,R*)-**5** (Figure 4b) and is typical for an autocatalytic process. The dimeric hemiacetal (*R,R,R,R*)-**8** represents a “super” diastereo-



Scheme 3. Proposed mechanism of the Soai-reaction with the formation of the transient Zn-hemiacetalate catalyst **5** as key step intermediate. All structures identified by the in situ high-resolution mass spectrometric experiments were considered in the mechanism. The green and red reaction arrows show the pathways to the reaction products, the dimers **3**, via Zn-hemiacetalate catalysis. R = $\text{C}\equiv\text{C}(\text{CH}_3)_3$.

meric complex and in combination with the dissociation into the monomeric hemiacetals (*R,R*)-**5**, which can dynamically control the stereocenter of the hemiacetal group, gives a natural mechanism of autocorrection. It has to be noted that (*R,R,R*)-**7** can be also directly converted into (*R,R*)-**5** and (*R*)-**2** (and its corresponding dimer (*R,R*)-**3**).

For the evaluation of the kinetic data we developed three kinetic models (models I, II and III) with increasing complexity (Figures S71–S73 in the Supporting Information). The minimal model (I) (Figure S71 in the Supplementary Information, 7 reaction steps) considers only a single enantiomer, the extended model (II) (Figure S72 in the Supporting Information) considers both enantiomers, and the comprehensive model (III) (Figure S73 in the Supporting Information) takes the epimeric hemiacetals **5** into account. It has to be pointed out that all three models result in consistent intrinsic reaction rates. The comprehensive model III consists of 26 differential equations (see Supporting Information for details) based on the here presented mechanism (Scheme 3) was created and implemented in a software program (Soai 7).^[56] This program allows to calculate kinetic reaction profiles using an adaptive Runge–Kutta routine to solve the system of differential equations with the initial experimental parameters, that is, concentrations of the additives (*R*)-**1** and (*S*)-**1** (*ee*), the pyrimidin-5-carbaldehyde **4** and *i*Pr₂Zn, the reaction time, reaction rate constants k_n (Scheme 3) and equilibrium constants K_n . This program allows to define large data sets (2.25 million kinetic profiles each) with variable ranges for the reaction rate constants k_n and equilibrium constants K_n . The calculated kinetic profiles are compared with the experimentally determined kinetic profiles

of (*R*)-**1**, (*S*)-**1** and **4** (Figure 1 b and Figures S6–S23 in the Supporting Information) to refine the kinetic parameters. This method was applied iteratively to all kinetic data sets (in total 81 million kinetic profiles) and thus the rate constants for the respective partial steps were determined (Figures S79–S100 in the Supporting Information). The kinetic and thermodynamic parameters are summarized in Table 2.

The formation of the isopropylzinc pyrimidyl alkoxides **2** is a rapid process and agrees very well with kinetic data of the reaction of alkylzinc compounds with alcohols.^[57] The equilibrium between monomeric **2** and homochiral (*R,R*)-**3**/*(S,S)*-**3** and heterochiral (*R,S*)-**3** is dynamic and not extremely shifted to the side of the dimers, as it is also observed in the mass spectra

Table 2. Kinetic data of the Soai-reaction of aldehyde **4** with *i*Pr₂Zn forming alcohol **1** obtained by comprehensive simulation of the proposed reaction mechanism

| $n^{[a]}$ | $k_n^{[b]}$ | $K_n^{[c]}$ | $k_{-n}^{[d]}$ |
|-----------|--|----------------------------|---|
| 1 | $1.5 \times 10^2 \pm 7 \text{ M}^{-1} \text{ s}^{-1}$ | | |
| 2 | $7.0 \times 10^2 \pm 32 \text{ M}^{-1} \text{ s}^{-1}$ | $81 \pm 4 \text{ M}^{-1}$ | $8.6 \pm 0.8 \text{ s}^{-1}$ |
| 3 | $7.0 \times 10^2 \pm 32 \text{ M}^{-1} \text{ s}^{-1}$ | $162 \pm 8 \text{ M}^{-1}$ | $4.3 \pm 0.4 \text{ s}^{-1}$ |
| 4 | 1.7×10^{-3} | 0.136 | 1.3×10^{-2} |
| | $\pm 1.2 \times 10^{-4} \text{ M}^{-1} \text{ s}^{-1}$ | $\pm 0.001 \text{ M}^{-1}$ | $\pm 1.0 \times 10^{-3} \text{ s}^{-1}$ |
| 5 | $63 \pm 5 \text{ M}^{-2} \text{ s}^{-1}$ | | |
| 6 | $0.11 \pm 0.01 \text{ s}^{-1}$ | | |
| 7 | $13.2 \pm 0.2 \text{ M}^{-1} \text{ s}^{-1}$ | | |
| 8 | $0.23 \pm 0.02 \text{ s}^{-1}$ | | |

[a] Reaction step as denoted in Scheme 3. [b] Forward reaction rate constants. [c] Equilibrium constants. [d] Backward reaction rate constants

(Figure 3 a). More interesting is the equilibrium and the kinetic parameters of the hemiacetal **5** formation, which are in excellent agreement with the kinetic parameters determined by enantioselective DHPLC (Figure 2 a–c) for the formation of **5**_{Pr} ($k_1(293\text{ K}) = 4.1 \times 10^{-3} (\text{mol s})^{-1}$ and $k_{-1}(293\text{ K}) = 1.3 \times 10^{-2} \text{ s}^{-1}$) and equilibria of the derivatives by ^1H NMR spectroscopy. In the autocatalytic cycle the rate determining step is the transfer of the isopropyl group, while the other steps are energetically balanced.

The proposed mechanism and the kinetic model allow not only to predict kinetic reaction profiles of the conversion of the pyrimidine-5-carbaldehyde **4** into the reaction product **1** of the Soai reaction, but even more important the precise prediction of the nonlinear amplification of the *ee* and the induction period in dependence on the *ee*. When starting with an *ee* of 1% in **1** (2 mmol/L), 9.25% *ee* in the 1st step, 59.4% *ee* in the 2nd step, 94.6% *ee* in the 3rd step, 99.4% *ee* in the 4th step and 99.9% *ee* in the 5th step are obtained (Figures S101–S105 of the Supporting Information). A systematic variation of the initial *ee*₀ of **1** and the corresponding final product *ee* is plotted in Figure 6 a (the corresponding final *ee* simulations are plotted in Figures S106–S115 in the Supporting Information). Interestingly, if the reaction is performed under conditions, where the formed product with amplifying *ee* propagates through a reaction mixture, that is, by diffusion or starting with seeding on a chiral or enantiomorph surface, extraordinary *ee* amplifications can be predicted, jumping immediately from $1 \times 10^{-5}\%$ to 55% and finally $> 99.9\%$ (Figure 6 a; red line). Experimental investigations of reactions with variation of the starting *ee* of the alcohol additive and concentrations were compared with the prediction of *ee* values by simulation with the program Soai 7, giving an excellent correlation between experiment and simulation (see Supporting Information Table S5 and Figure S117).

Furthermore, the simulations correctly predict the prolonged induction period, which is caused by the slow hemiacetal formation, and the time of the inflection point t_{ip} in dependence on the initial *ee* of the pyrimidine alcohol **1** (Figure 6 b).

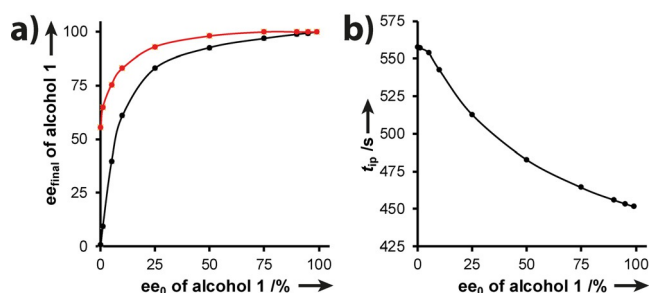


Figure 6. Enantiomeric excess and time of the inflection point in dependence on the initial *ee* of the added pyrimidine alcohol **1** predicted by the mechanistic model and reaction rate constants obtained by comprehensive analysis of the kinetic data. Simulations were obtained by calculations with Soai 7. a) Amplification of the *ee* (final *ee* vs. initial *ee* of the alcohol **1**). The black line represents a homogeneous and stirred reaction mixture, the red line represents a Soai reaction slowly propagating through a reaction mixture. b) Shift of the inflection point t_{ip} in dependence on the initial *ee* of **1**. Starting concentrations used for simulation: 25.0 mM **4**, 2 mM **1** (ratio of (*R*)-**1** and (*S*)-**1** depending on the corresponding *ee*) and 50 mM *i*Pr₂Zn.

Conclusions

In summary, the results of the high-resolution mass spectrometric measurements and the comprehensive kinetic analyses suggest the formation of a transient Zn–hemiacetalate complex, which is catalytically active in the Soai reaction. This intermediate can establish the here proposed autocatalytic cycle and the extraordinary amplification of the enantiomeric excess. This is supported by mass spectrometric profiling of the transient hemiacetal intermediate and by doping experiments, which demonstrate that the Soai reaction can be accelerated by adding the in situ formed catalyst. Kinetic and thermodynamic data of the highly dynamic formation and decomposition of the hemiacetal explain the unusual inverse temperature dependence on the reaction kinetics, the induction period and time shift of the inflection point. Furthermore, the results suggest that the formation of the transient diastereomeric Zn–hemiacetalates amplify any initial imbalance of the formed product enantiomers, which is interestingly always given for an odd number of formed molecules. These results give a new guidance to structures envisioning potential processes leading to symmetry breaking.

Acknowledgements

We acknowledge financial support from the European Research Council ERC under Grant Agreements No. StG 258740, the Ludwig-Maximilians-University Munich, the Max-Planck-Society (Max-Planck-Fellow Research Group Origins of Life) and the Deutsche Forschungsgemeinschaft DFG (INST 86/1807-1 FUGG). Open access funding enabled and organized by Projekt DEAL.

Conflict of interest

The authors declare no conflict of interest.

Keywords: autocatalysis · hemiacetal · kinetic analysis · mass spectrometry · Soai reaction

- [1] a) J.-M. Lehn, *Angew. Chem. Int. Ed.* **2013**, *52*, 2836–2850; *Angew. Chem.* **2013**, *125*, 2906–2921; b) J.-M. Lehn, *Angew. Chem. Int. Ed.* **2015**, *54*, 3276–3289; *Angew. Chem.* **2015**, *127*, 3326–3340.
[2] D. G. Blackmond, *Chem. Rev.* **2020**, *120*, 4831–4847.
[3] a) I. Weissbuch, L. Addadi, Z. Berkovitch-Yellin, E. Gati, M. Lahav, L. Leiserowitz, *Nature* **1984**, *310*, 161–164; b) D. K. Kondepudi, R. J. Kaufman, N. Singh, *Science* **1990**, *250*, 975–976; c) B. L. Feringa, R. A. van Delden, *Angew. Chem. Int. Ed.* **1999**, *38*, 3418–3438; *Angew. Chem.* **1999**, *111*, 3624–3645; d) H. Zepik, E. Shavit, M. Tang, T. R. Jensen, K. Kjaer, G. Bolbach, L. Leiserowitz, I. Weissbuch, M. Lahav, *Science* **2002**, *295*, 1266; e) K. Mikami, M. Yamanaka, *Chem. Rev.* **2003**, *103*, 3369–3400; f) D. G. Blackmond, *Proc. Natl. Acad. Sci. USA* **2004**, *101*, 5732–5736; g) R. R. E. Steendam, M. C. T. Brouwer, E. M. E. Huijs, M. W. Kulka, H. Meekes, W. J. P. V. Enckevort, J. Raap, F. P. J. T. Rutjes, E. Vlieg, *Chem. Eur. J.* **2014**, *20*, 13527–13530; h) S. Olsson, P. M. Björemark, T. Kokoli, J. Sundberg, A. Lennartson, C. J. McKenzie, M. Häkansson, *Chem. Eur. J.* **2015**, *21*, 5211–5219; i) J. M. Ribo, J. Crusats, Z. El-Hachemi, A. Moyano, D. Hochberg, *Chem. Sci.* **2017**, *8*, 763–769.

- [4] a) D. Guillaneux, S.-H. Zhao, O. Samuel, D. Rainford, H. B. Kagan, *J. Am. Chem. Soc.* **1994**, *116*, 9430–9439; b) C. Girard, H. B. Kagan, *Angew. Chem. Int. Ed.* **1998**, *37*, 2922–2959; *Angew. Chem.* **1998**, *110*, 3088–3127; c) M. Klussmann, H. Iwamura, S. P. Mathew, D. H. Wells, U. Pandya, A. Armstrong, D. G. Blackmond, *Nature* **2006**, *441*, 621–623; d) T. Satyanarayana, S. Abraham, H. B. Kagan, *Angew. Chem. Int. Ed.* **2009**, *48*, 456–494; *Angew. Chem.* **2009**, *121*, 464–503; e) D. G. Blackmond, *Tetrahedron: Asymmetry* **2010**, *21*, 1630–1634; f) S. B. Tsogoeva, *Chem. Commun.* **2010**, *46*, 7662–7669.
- [5] C. Puchot, O. Samuel, E. Duijich, S. Zhao, C. Agami, H. B. Kagan, *J. Am. Chem. Soc.* **1986**, *108*, 2353–2357.
- [6] a) M. Kitamura, S. Okada, S. Suga, R. Noyori, *J. Am. Chem. Soc.* **1989**, *111*, 4028–4036; b) R. Noyori, M. Kitamura, *Angew. Chem. Int. Ed. Engl.* **1991**, *30*, 49–69; *Angew. Chem.* **1991**, *103*, 34–55.
- [7] K. Soai, S. Niwa, *Chem. Rev.* **1992**, *92*, 833–856.
- [8] F. C. Frank, *Biochim. Biophys. Acta* **1953**, *11*, 459–463.
- [9] M. E. Noble-Terán, T. Buhse, J.-M. Cruz, C. Coudret, J.-C. Micheau, *ChemCatChem* **2016**, *8*, 1836–1845.
- [10] a) K. Soai, T. Shibata, H. Morioka, K. Choji, *Nature* **1995**, *378*, 767–768; b) K. Soai, T. Shibata, *J. Synth. Org. Chem. Jpn.* **1997**, *55*, 994–1005; c) T. Shibata, S. Yonekubo, K. Soai, *Angew. Chem. Int. Ed.* **1999**, *38*, 659–661; *Angew. Chem.* **1999**, *111*, 746–748; d) K. Soai, T. Shibata, I. Sato, *Acc. Chem. Res.* **2000**, *33*, 382–390.
- [11] Reviews: a) K. Soai, T. Kawasaki, *Chirality* **2006**, *18*, 469–478; b) K. Soai, T. Kawasaki, *Top. Curr. Chem.* **2008**, *284*, 1–33; c) T. Gehring, M. Busch, M. Schlageter, D. Weingand, *Chirality* **2010**, *22*, E173–E182.
- [12] a) K. Soai, S. Niwa, H. Hori, *J. Chem. Soc. Chem. Commun.* **1990**, 982–983; b) T. Shibata, K. Choji, T. Hayase, Y. Aizu, K. Soai, *Chem. Commun.* **1996**, 1235–1236; c) K. Soai, T. Sato, *Chirality* **2002**, *14*, 548–554; d) C. Romagnoli, B. Sieng, M. Amedjkouh, *Eur. J. Org. Chem.* **2015**, 4087–4092.
- [13] a) D. A. Singleton, L. K. Vo, *J. Am. Chem. Soc.* **2002**, *124*, 10010–10011; b) D. A. Singleton, L. K. Vo, *Org. Lett.* **2003**, *5*, 4337–4339.
- [14] I. Sato, H. Urabe, S. Ishiguro, T. Shibata, K. Soai, *Angew. Chem. Int. Ed.* **2003**, *42*, 315–317; *Angew. Chem.* **2003**, *115*, 329–331.
- [15] a) I. Sato, D. Omiya, T. Saito, K. Soai, *J. Am. Chem. Soc.* **2000**, *122*, 11739–11740; b) T. Kawasaki, M. Shimizu, D. Nishiyama, M. Ito, H. Ozawa, K. Soai, *Chem. Commun.* **2009**, 4396–4398; c) T. Kawasaki, H. Ozawa, M. Ito, K. Soai, *Chem. Lett.* **2011**, *40*, 320–321.
- [16] T. Kawasaki, Y. Matsumura, T. Tsutsumi, K. Suzuki, M. Ito, K. Soai, *Science* **2009**, *324*, 492–495.
- [17] A. Matsumoto, H. Ozaki, S. Harada, K. Tada, T. Ayugase, H. Ozawa, T. Kawasaki, K. Soai, *Angew. Chem. Int. Ed.* **2016**, *55*, 15246–15249; *Angew. Chem.* **2016**, *128*, 15472–15475.
- [18] a) T. Kawasaki, Y. Okano, E. Suzuki, S. Takano, S. Oji, K. Soai, *Angew. Chem. Int. Ed.* **2011**, *50*, 8131–8133; *Angew. Chem.* **2011**, *123*, 8281–8283; b) A. Matsumoto, S. Oji, S. Takano, K. Tada, T. Kawasaki, K. Soai, *Org. Biomol. Chem.* **2013**, *11*, 2928–2931.
- [19] N. A. Hawbaker, D. G. Blackmond, *ACS Cent. Sci.* **2018**, *4*, 776–780.
- [20] T. Kawasaki, H. Tanaka, T. Tsutsumi, T. Kasahara, I. Sato, K. Soai, *J. Am. Chem. Soc.* **2006**, *128*, 6032–6033.
- [21] a) I. Sato, R. Sugie, Y. Matsueda, Y. Furumura, K. Soai, *Angew. Chem. Int. Ed.* **2004**, *43*, 4490–4492; *Angew. Chem.* **2004**, *116*, 4590–4592; b) T. Kawasaki, M. Sato, S. Ishiguro, T. Saito, Y. Morishita, I. Sato, H. Nishino, Y. Inoue, K. Soai, *J. Am. Chem. Soc.* **2005**, *127*, 3274–3275.
- [22] a) K. Soai, S. Osanai, K. Kadowaki, S. Yonekubo, T. Shibata, I. Sato, *J. Am. Chem. Soc.* **1999**, *121*, 11235–11236; b) I. Sato, K. Kadowaki, K. Soai, *Angew. Chem. Int. Ed.* **2000**, *39*, 1510–1512; *Angew. Chem.* **2000**, *112*, 1570–1572; c) T. Kawasaki, K. Jo, H. Igarashi, I. Sato, M. Nagano, H. Koshima, K. Soai, *Angew. Chem. Int. Ed.* **2005**, *44*, 2774–2777; *Angew. Chem.* **2005**, *117*, 2834–2837; d) T. Kawasaki, K. Suzuki, M. Shimizu, K. Ishikawa, K. Soai, *Chirality* **2006**, *18*, 479–482; e) T. Kawasaki, K. Suzuki, Y. Hakoda, K. Soai, *Angew. Chem. Int. Ed.* **2008**, *47*, 496–499; *Angew. Chem.* **2008**, *120*, 506–509; f) T. Kawasaki, S. Kamimura, A. Amihara, K. Suzuki, K. Soai, *Angew. Chem. Int. Ed.* **2011**, *50*, 6796–6798; *Angew. Chem.* **2011**, *123*, 6928–6930; g) H. Shindo, Y. Shirota, K. Niki, T. Kawasaki, K. Suzuki, Y. Araki, A. Matsumoto, K. Soai, *Angew. Chem. Int. Ed.* **2013**, *52*, 9135–9138; *Angew. Chem.* **2013**, *125*, 9305–9308; h) H. Mineki, Y. Kaimori, T. Kawasaki, A. Matsumoto, K. Soai, *Tetrahedron: Asymmetry* **2013**, *24*, 1365–1367; i) T. Kawasaki, M. Uchida, Y. Kaimori, T. Sasagawa, A. Matsumoto, K. Soai, *Chem. Lett.* **2013**, *42*, 711–713; j) A. Matsumoto, T. Ide, Y. Kaimori, S. Fujiwara, K. Soai, *Chem. Lett.* **2015**, *44*, 688–690; k) A. Matsumoto, S. Takeda, S. Harada, K. Soai, *Tetrahedron: Asymmetry* **2016**, *27*, 943–946.
- [23] a) F. Lutz, T. Kawasaki, K. Soai, *Tetrahedron: Asymmetry* **2006**, *17*, 486–490; b) T. Kawasaki, C. Hohberger, Y. Araki, K. Hatase, K. Beckerle, J. Okuda, K. Soai, *Chem. Commun.* **2009**, 5621–5623; c) G. A. Rance, S. A. Miners, T. W. Chamberlain, A. N. Khlobystov, *Chem. Mater.* **2013**, *25*, 10–14; d) T. Kawasaki, M. Nakaoda, Y. Takahashi, Y. Kanto, N. Kuruwara, K. Hosoi, I. Sato, A. Matsumoto, K. Soai, *Angew. Chem. Int. Ed.* **2014**, *53*, 11199–11202; *Angew. Chem.* **2014**, *126*, 11381–11384; e) C. J. Welch, K. Zawatzky, A. A. Makarov, S. Fujiwara, A. Matsumoto, K. Soai, *Org. Biomol. Chem.* **2017**, *15*, 96–101; f) A. Matsumoto, K. Yonemitsu, H. Ozaki, J. Misek, I. Stary, I. G. Stara, K. Soai, *Org. Biomol. Chem.* **2017**, *15*, 1321–1324.
- [24] K. Soai, I. Sato, T. Shibata, S. Komiya, M. Hayashi, Y. Matsueda, H. Imaura, T. Hayase, H. Morioka, H. Tabira, J. Yamamoto, Y. Kowata, *Tetrahedron: Asymmetry* **2003**, *14*, 185–188.
- [25] J. M. Brown, I. Gridnev, J. Klankermayer, *Top. Curr. Chem.* **2008**, *284*, 35–65.
- [26] a) K. Micskei, G. Póta, L. Caglioti, G. Pályi, *J. Phys. Chem. A* **2006**, *110*, 5982–5984; b) D. G. Blackmond, O. K. Matar, *J. Phys. Chem. B* **2008**, *112*, 5098–5104; c) G. Lente, *Tetrahedron: Asymmetry* **2011**, *22*, 1595–1599; d) J.-C. Micheau, C. Coudret, J.-M. Cruz, T. Buhse, *Phys. Chem. Chem. Phys.* **2012**, *14*, 13239–13248; e) B. Barabás, C. Zucchi, M. Maioli, K. Micskei, G. Pályi, *J. Mol. Model.* **2015**, *21*, 33; f) I. D. Gridnev, A. K. Vorobiev, *ACS Catal.* **2012**, *2*, 2137–2149.
- [27] I. D. Gridnev, A. K. Vorobiev, *Bull. Chem. Soc. Jpn.* **2015**, *88*, 333–340.
- [28] a) J. R. Islas, D. Lavabre, J.-M. Grevy, R. H. Lamonedá, H. R. Cabrera, J.-C. Micheau, T. Buhse, *Proc. Natl. Acad. Sci. USA* **2005**, *102*, 13743–13748; b) J.-C. Micheau, J.-M. Cruz, C. Coudret, T. Buhse, *ChemPhysChem* **2010**, *11*, 3417–3419.
- [29] J. Podlech, T. Gehring, *Angew. Chem. Int. Ed.* **2005**, *44*, 5776–5777; *Angew. Chem.* **2005**, *117*, 5922–5924.
- [30] F. G. Buono, D. G. Blackmond, *J. Am. Chem. Soc.* **2003**, *125*, 8978–8979.
- [31] I. D. Gridnev, J. M. Serafimov, H. Quiney, J. M. Brown, *Org. Biomol. Chem.* **2003**, *1*, 3811–3819.
- [32] D. G. Blackmond, C. R. McMillan, S. Ramdeehul, A. Schorm, J. M. Brown, *J. Am. Chem. Soc.* **2001**, *123*, 10103–10104.
- [33] D. G. Blackmond, *Tetrahedron: Asymmetry* **2006**, *17*, 584–589.
- [34] J. Klankermayer, I. D. Gridnev, J. M. Brown, *Chem. Commun.* **2007**, 3151–3153.
- [35] A. Matsumoto, T. Abe, A. Hara, T. Tobita, T. Sasagawa, T. Kawasaki, K. Soai, *Angew. Chem. Int. Ed.* **2015**, *54*, 15218–15221; *Angew. Chem.* **2015**, *127*, 15433–15436.
- [36] I. D. Gridnev, J. M. Serafimov, J. M. Brown, *Angew. Chem. Int. Ed.* **2004**, *43*, 4884–4887; *Angew. Chem.* **2004**, *116*, 4992–4995.
- [37] M. Busch, M. Schlageter, D. Weingand, T. Gehring, *Chem. Eur. J.* **2009**, *15*, 8251–8258.
- [38] a) L. Schiaffino, G. Ercolani, *Angew. Chem. Int. Ed.* **2008**, *47*, 6832–6835; *Angew. Chem.* **2008**, *120*, 6938–6941; b) L. Schiaffino, G. Ercolani, *ChemPhysChem* **2009**, *10*, 2508–2515; c) L. Schiaffino, G. Ercolani, *Chem. Eur. J.* **2010**, *16*, 3147–3156; d) G. Ercolani, L. Schiaffino, *J. Org. Chem.* **2011**, *76*, 2619–2626.
- [39] T. Gehring, M. Quaranta, B. Odell, D. G. Blackmond, J. M. Brown, *Angew. Chem. Int. Ed.* **2012**, *51*, 9539–9542; *Angew. Chem.* **2012**, *124*, 9677–9680.
- [40] S. V. Athavale, A. Simon, K. N. Houk, S. E. Denmark, *Nat. Chem.* **2020**, *12*, 412–423.
- [41] M. Quaranta, T. Gehring, B. Odell, J. M. Brown, D. G. Blackmond, *J. Am. Chem. Soc.* **2010**, *132*, 15104–15107.
- [42] a) O. Trapp, *Angew. Chem. Int. Ed.* **2007**, *46*, 5609–5613; *Angew. Chem.* **2007**, *119*, 5706–5710; b) A. F. Siegle, O. Trapp, *Anal. Chem.* **2014**, *86*, 10828–10833; c) A. F. Siegle, O. Trapp, *Anal. Chem.* **2015**, *87*, 11932–11934.
- [43] C. J. Welch, X. Gong, W. Schafer, E. C. Pratt, T. Brkovic, Z. Pirzada, J. F. Cuff, B. Kosjek, *Tetrahedron: Asymmetry* **2010**, *21*, 1674–1681.
- [44] a) O. Trapp, G. Schoetz, V. Schurig, *Chirality* **2001**, *13*, 403–414; b) I. D'Acquarica, F. Gasparini, M. Pierini, C. Villani, G. Zappia, *J. Sep. Sci.* **2006**, *29*, 1508–1516; c) C. Wolf, *Dynamic Stereochemistry of Chiral Compounds—Principles and Applications*, RSC Publishing, Cambridge, **2008**; d) O. Trapp, *Top. Curr. Chem.* **2013**, *341*, 231–270.

- [45] a) O. Trapp, V. Schurig, *J. Am. Chem. Soc.* **2000**, *122*, 1424–1430; b) O. Trapp, *Anal. Chem.* **2006**, *78*, 189–198; c) O. Trapp, *Electrophoresis* **2006**, *27*, 534–541; d) O. Trapp, *Electrophoresis* **2006**, *27*, 2999–3006; e) F. Maier, O. Trapp, *Angew. Chem. Int. Ed.* **2012**, *51*, 2985–2988; *Angew. Chem.* **2012**, *124*, 3039–3043.
- [46] a) H. Fanlo-Virgós, A.-N. R. Alba, S. Hamieh, M. Colomb-Delsuc, S. Otto, *Angew. Chem. Int. Ed.* **2014**, *53*, 11346–11350; *Angew. Chem.* **2014**, *126*, 11528–11532; b) C. Kremer, A. Lützen, *Chem. Eur. J.* **2013**, *19*, 6162–6196.
- [47] a) E. Wingstrand, A. Laurell, L. Fransson, K. Hult, C. Moberg, *Chem. Eur. J.* **2009**, *15*, 12107–12113; b) L. Fransson, C. Moberg, *ChemCatChem* **2010**, *2*, 1523–1532; c) L. Fransson, A. Laurell, K. Widyana, E. Wingstrand, K. Hult, C. Moberg, *ChemCatChem* **2010**, *2*, 683–693; d) A. Laurell, C. Moberg, *Eur. J. Org. Chem.* **2011**, 3980–3984; e) Y.-Q. Wen, R. Hertzberg, I. Gonzalez, C. Moberg, *Chem. Eur. J.* **2014**, *20*, 3806–3812; f) C. Moberg, *Acc. Chem. Res.* **2016**, *49*, 2736–2745.
- [48] M. Funes-Maldonado, B. Sieng, M. Amedjkouh, *Eur. J. Org. Chem.* **2015**, 4081–4086.
- [49] C. Adamo, V. Barone, *Chem. Phys. Lett.* **1998**, *298*, 113–119.
- [50] a) J. P. Perdew, K. Burke, M. Ernzerhof, *Phys. Rev. Lett.* **1996**, *77*, 3865–3868; b) J. P. Perdew, K. Burke, M. Ernzerhof, *Phys. Rev. Lett.* **1997**, *78*, 1396.
- [51] S. Grimme, E. Antony, T. Ehrlich, E. Krieg, *J. Chem. Phys.* **2010**, *132*, 154104.
- [52] P. J. Hay, I. R. Wadt, *J. Chem. Phys.* **1985**, *82*, 299–310.
- [53] P. C. Hariharan, J. A. Pople, *Theor. Chim. Acta* **1973**, *28*, 213–222.
- [54] Jaguar, version 10.1, Schrodinger, Inc., New York, NY, 2018.
- [55] A. D. Bochevarov, E. Harder, T. F. Hughes, J. R. Greenwood, D. A. Braden, D. M. Philipp, D. Rinaldo, M. D. Halls, J. Zhang, R. A. Friesner, *Int. J. Quantum Chem.* **2013**, *113*, 2110–2142.
- [56] O. Trapp, Soai 7, compatible with Microsoft Windows 7, 8 and 10. The compiled executable program can be obtained from the author upon request.
- [57] R. J. Herold, S. L. Aggarwal, V. Neff, *Can. J. Chem.* **1963**, *41*, 1368–1380.

Manuscript received: July 13, 2020

Accepted manuscript online: August 21, 2020

Version of record online: October 15, 2020